Jour. Geol. Soc. India (2022) 98:219-231
https://doi.org/10.1007/s12594-022-1962-9

ORIGINAL ARTICLE

Petrography and Geochemistry of Sandstones of Eocene Kopili Formation, Shillong Plateau: Implications on Paleo-weathering, Provenance and Tectonic Setting

Poly Sonowal[1], Tavheed Khan[2], Mousumi Gogoi[1], T. Satish Kumar[3], Temsulemba Walling[4] and Sarat Phukan[1,*]

[1]Department of Geological Sciences, Gauhati University, Guwahati - 781 014, India
[2]Geochemistry Division, CSIR-National Geophysical Research Institute, Hyderabad - 500 007, India
[3]Centre of Excellence for Energy Studies, Oil India Ltd., Guwahati - 781 022, India
[4]Department of Geology, Nagaland University, Kohima - 797 004, India
E-mail: *polysonowal96@gmail.com; khan.tauheedgeo23@gmail.com; mv.mousumi@gauhati.ac.in; satishthadoju@gmail.com; temsuwalling@nagalanduniversity.ac.in; saratphukan@gauhati.ac.in**

Received: 11 February 2021/ Revised form Accepted: 26 June 2021

ABSTRACT

Geochemical and mineralogical studies were carried out on the sandstones of the Eocene Kopili Formation, Shillong Plateau to evaluate paleo-weathering, provenance and tectonic setting. The study area is located on the bank of the Lubha River along the Badarpur-Jowai road section. The Kopili Formation is represented by a sequence of alternation of shales and sandstones. The sandstone beds are usually thin, fine grained, ferruginous and mostly parallel laminated. The thickness of the sandstone beds increases towards the top with decreasing numbers of shale beds. Petrographically the sandstones are dominated by monocrystalline and polycrystalline quartz followed by feldspar, mica and rock fragments. The matrix content does not exceed 15% and hence the sandstones can be classified as arenite. The Kopili sandstones are classified as quartz arenite to sublitharenite, and arkose to sublitharenite based on their petrographic and geochemical parameters respectively. Arenitic composition and high SiO_2/Al_2O_3 ratio indicate that the Kopili sandstones are highly mature. The weathering indices mostly indicate low to moderate (except 49D sample) degree of chemical weathering under arid to semi humid climatic conditions. The major and trace element-based diagrams and their ratios indicate that the Kopili sandstone received sediments from felsic dominated source with minor contribution from basic source rocks and are deposited in tectonically passive margin setting.

INTRODUCTION

Geochemical study of clastic sedimentary rocks yields valuable information about sediment generation, transportation, paleoclimate, degree of weathering and tectonic setting (e.g., Nesbitt et al., 1980; Nesbit and Young, 1982; Bhatia, 1983; Taylor and McLennan, 1985; Bhatia and Crook, 1986; Roser and Korsch, 1986; Dabard, 1990; McLennan et al., 1990, Armstrong-Altrin et al., 2004; Ghosh et al., 2012; Hara et al., 2012, Armstrong-Altrin et al. 2013). The trace element and REE distribution patterns are important in understanding provenance and tectonic settings of sedimentary basins because of their immobility and short residence time in seawater (Periasamy and Venkateshwarlu, 2017). Major element distribution pattern in sandstones also provide valuable information on tectonic setting, if the bulk composition of the sediments is not altered (Bhatia, 1983; Roser and Korsch, 1986; McLennan, 1989; Nesbitt and Young, 1989). Tectonic discrimination diagrams of Bhatia (1983), and Roser and Korsch (1986) have been in use for deciphering tectonic settings of sedimentary basins. In addition to geochemical methods, detailed petrographic methods have also been developed for studying paleoclimate, provenance and tectonic evolution of sedimentary basins (Crook, 1974; Dickinson and Suczek, 1979; Dickinson et al., 1983). However, because of submicroscopic size of the mineral grains of argillites and siltstones, the petrographic methods are mostly suitable for sandstones only. This restriction does not apply to bulk chemical data (Roser and Korsch, 1986). The bulk geochemical data can supplement petrographic analysis in understanding processes that involved in generation of sediments and evolution of sedimentary basins.

Evans (1932) classified Eocene shaly sequence overlying the 'Sylhet Limestone Stage' in the south Shillong plateau as Kopili Alteration Stage. Both were originally part of the 'Nummulitic Series' of Medlicott (1869). Chakraborty et al. (1974) and Bhandari et al. (1973) based on lithological characters has considered it as a Formation. The type section is present along the Kopili River section near Khorungma (Evans, 1932). The exposures of the Kopili Formation are present all over the south Shillong Plateau. It is also exposed along the southern fringe of the Karbi Anglong Massif and present in the subsurface of the Assam Shelf (Reddy et al., 1992). It gradationally overlies the Sylhet Formation of Eocene age and conformably overlain by the Barail Group of Oligocene age. It is generally considered as a regressive sequence with the basal part of the formation considered to be deposited under inner shelf environment that gave way to brackish tide dominated environment in the upper part (Deshpande et al., 1993). The underlying Sylhet Formation is generally considered as a major transgressive phase in the Assam-Arakan Basin. The Kopili Formation is primarily composed of alterations of shale and sandstone. The age

of Kopili Formation is considered as late Eocene (Saxena and Trivedi, 2009).

Available literature on the Kopili exposures of the south Shillong Plateau are mostly on its foraminifera and palynofossil assemblages (Trivedi and Ranhotra, 2015; Samanta, 1968; Samanta, 1985; Dutta and Jain, 1980; Sein and Sah, 1974; Tripathi and Singh, 1984). Based on lithology of the subsurface shelf sequence of Assam Shelf, few studies have been carried out on depositional model of the Kopili Formation (Zaidi and Chakrabarti, 2006; Roy Moulik et al., 2009). However, notable sedimentological and geochemical studies on the sandstones of the Kopili Formation from the Shillong Plateau region are still rare. The aim of the present study is to investigate on provenance, weathering and tectonic setting of the Kopili Formation and evolution of the south Shillong Shelf during upper Eocene time by using petrography and, major and trace elements (including REEs) geochemistry.

GEOLOGY OF THE STUDY AREA

The study area is a part of Jaintia hills district of Meghalaya and bounded by 92°10'-92°25' E longitudes and 25°4'-25°12' N latitudes (Fig. 1). The stratigraphic succession of the study area is shown in the Table 1. The Kopili Formation is exposed on the bank of the Lubha River along Jowai-Badarpur road section (Fig. 2) near Sonapur. The Kopili Formation is the youngest formation of the Jaintia Group and comprises of alternation of fine to very fine grained compact, massive to laminated sandstone and splintery shale with thin streaks of coal. At few places, fossiliferous limestone and marls are also present at basal part. The study area rests on the monoclinal flexure of the Shillong plateau in the vicinity of the Dawki fault. The Kopili Formation conformably overlies the Prang Limestone Member of the Sylhet Formation. The top part of the Formation is truncated by a fault that runs along the Lubha River course which is possibly an offshoot of the Dawki fault system (Fig. 2). On the other bank of the Lubha River the top formation of the Oligocene Barail Group i.e., the Renji Formation is exposed. Thus, the Kopili and the Renji Formations have a faulted boundary. The beds of the Renji Formation are overturned, as shown by the orientation of ripple marks and cross beddings. The Kopili sandstone beds are usually thin (20-80cm), fine grained, ferruginous and parallel laminated. The thickness of the sandstone beds increases towards the top with decreasing numbers of shale beds. Shales are brown to grey, occasionally iron stained, hard and splintery. The rock beds have general dip of 30 to 56° towards northwest. The dip of the beds gradually decreases towards the north of the study area with as the monoclinal flexure disappears. The litholog of the Kopili Formation as exposed along the road is shown in Fig. 3.

MATERIALS AND METHODS

A total of thirty-four (34) representative sandstone samples of Kopili Formation were collected from the Jowai-Badarpur road section that exposes along the bank of the Lubha river. All these samples were studied under petrological microscope for petrographic discrimination. The detrital frame work grains of the Kopili sandstone

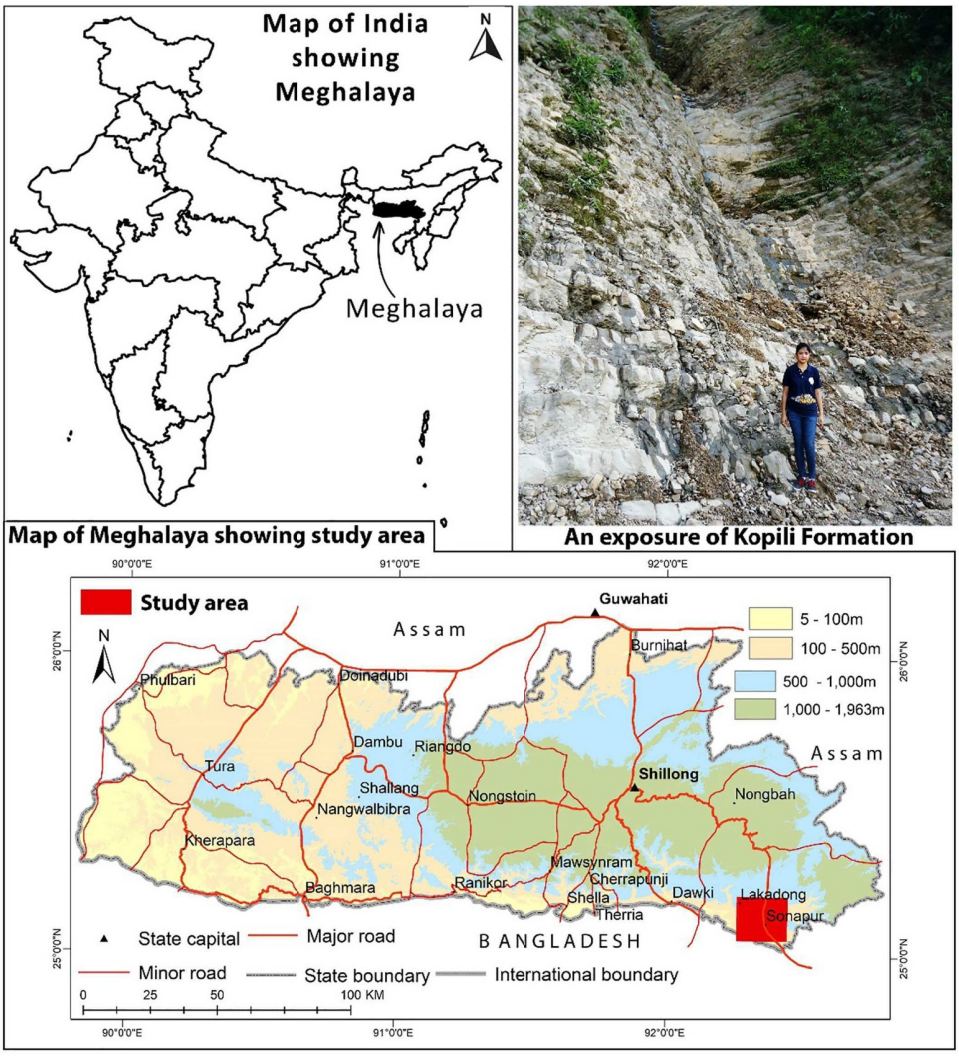

Fig. 1. Location map of the study area.

Table 1. Stratigraphic succession of the study area (modified after Deshpande et al., 1993)

Group	Formation	Member	Lithology	Age
Barail Group	Renji Formation		Feruginous and massive sandstone with thin shale and sandy shale interbeds. The sandstones are medium to fine grained, and show a coarsening upward sequence.	Late Oligocene
Disang Group	Kopili Formation		Alternations of shales and hard and fine-grained sandstones. Sandstones are ferruginous. Marl streaks are present at the base.	Late Eocene
	Sylhet Formation	Prang Limestone	Grey to greyish white, fossiliferous, massive and crystalline limestone. Sandy at the base.	Late Eocene
		Narpuh Sandstone	Dirty white, coarse grained medium to coarse grained quartzose sandstone. Calcareous grit and occasional thin limestone bands at the base.	Early Eocene
Base exposed outside study area				

were counted with the swift automatic point counter fitted in the petrographic microscope. About 300-500 grains were counted in each thin section. The modal analysis results are given in the Table 2. The nomenclature of the framework modes, their classification and tabulation are as per standards prescribed in Krynine (1940), Folk (1980), Basu et al. (1975) and Ingersoll et al. (1984). The major element analyses have been done for nineteen (19) samples with Philips MagiX PRO (Model PW 2440) sequential wavelength dispersive X-ray fluorescence spectrometer which is coupled with an automatic sample changer (PW 2540). The analyses of trace and rare earth elements of the same samples was performed by a high resolution inductively coupled plasma mass spectrometer (HR - ICP - MS; Nu Instruments Attom, UK) by following the in-house standard procedures at CSIR-National Geophysical Research Institute, Hyderabad. Rock standard GSR-4 was used to calibrate the instrument. Accuracy and precision protocols for major and trace elements have been developed by Krishna et al. (2007) and Satyanarayanan et al. (2014), respectively. The results of the geochemical analyses are given in the Table 3 and 4.

PETROGRAPHY

Quartz is the most dominant mineral in monocrystalline and polycrystalline forms (Fig. 4a & b) in the Kopili sandstones and its amount varies from 69.20 to 90.47% (avg. 81.83%) (Table 2). Some quartz grains show overgrowth (Fig. 4c). The proportion of feldspar

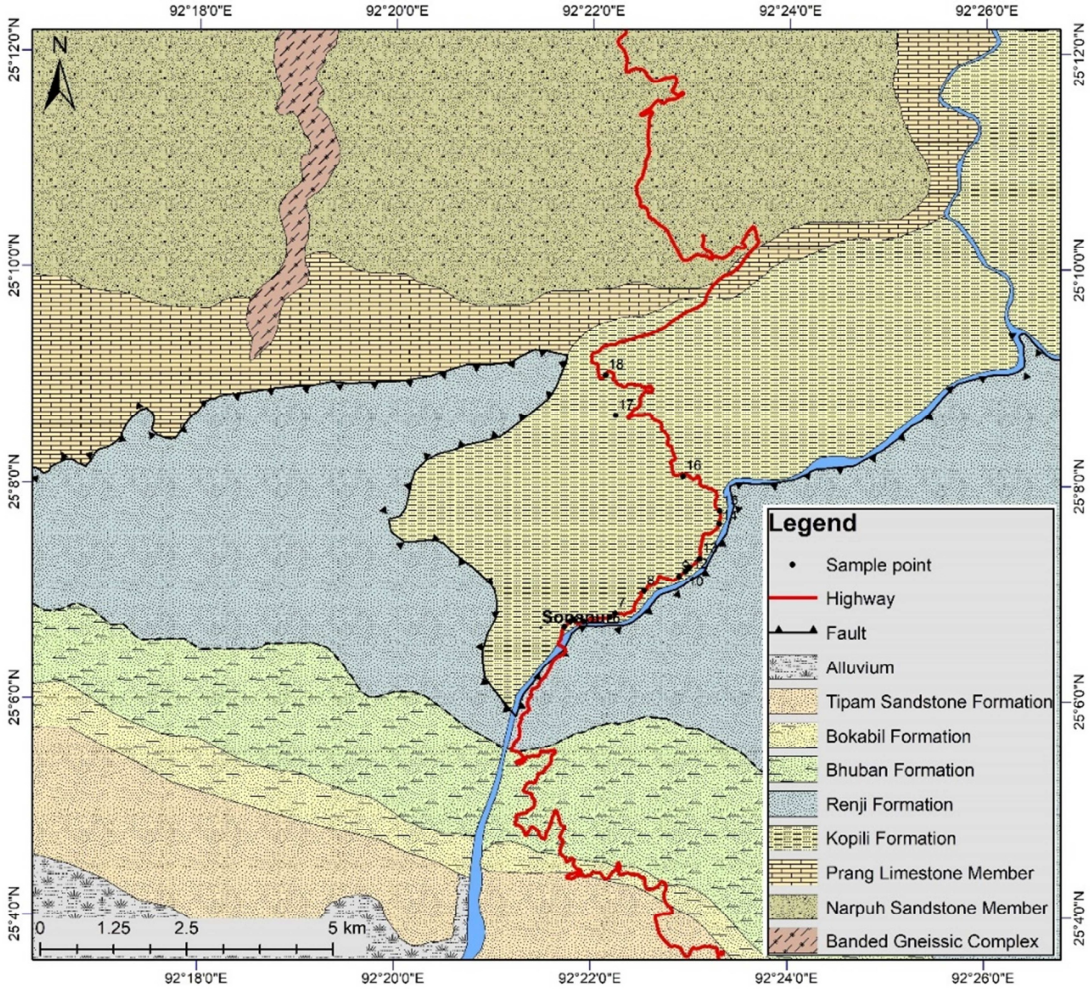

Fig. 2. Geological map of the study area.

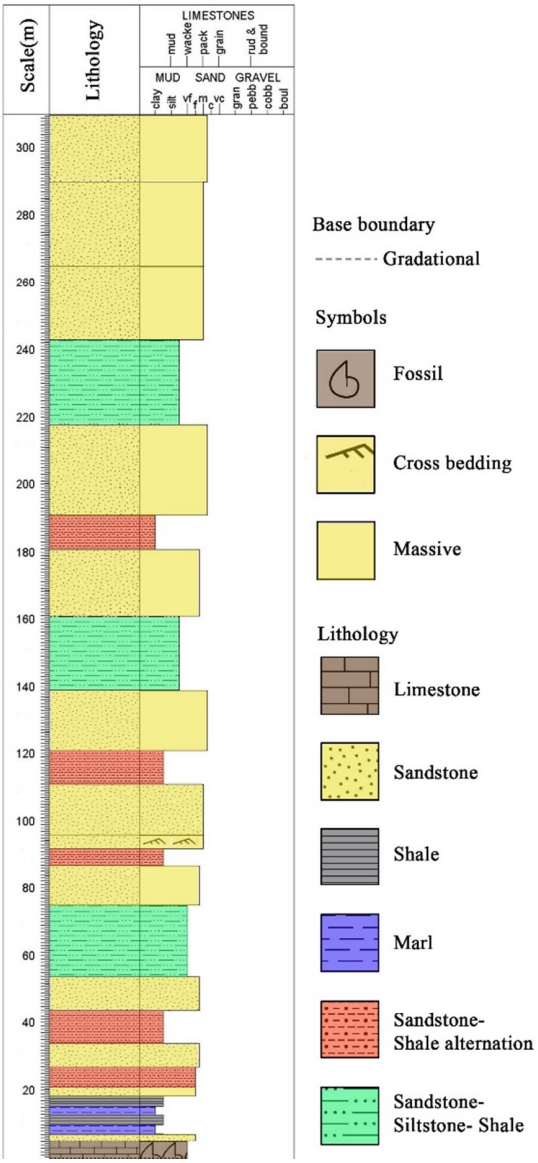

Fig. 3. Litholog of the Kopili Formation exposed on the bank of Lubha River, Jaintia Hills.

varies from 0.00 to 1.18% (avg. 0.45%) and represented by plagioclase and microcline (Fig. 4d & e) (Table 2). Mica ranges from 0.55 to 7.29% (avg. 3.41%) and represented mostly by muscovite (Fig. 4f) with a very minor fraction of biotite (Table 2). The percentage of rock fragments varies from 1.48 to 19.6% (avg 6.37%) (Table 2). The majority of the rock fragments are metamorphic (Fig. 5a) followed by sedimentary (Fig. 5b & c) and igneous rocks (Fig. 5d) in order of their abundance. Sedimentary rock fragments are mostly represented by shale fragments and cherts (Fig. 5b & c). Heavy minerals are mostly represented by zircon and tourmaline (Fig. 5e & f). Presence of zircon inclusions indicates their derivation from the plutonic igneous rock. Most of the grains are cemented by silica. Ferruginous cement is also common. Cementing material ranges from 1.84 to 8.53% by volume (Table 2). The matrix content in the Kopili sandstone varies from 1.0 to 8.10% (Table 2). Since matrix abundance in the Kopili sandstones does not exceed 15% by volume, they are classified as arenite (Pettijohn et al., 1987). To classify the sandstone the percentages of framework grains of the sandstones are plotted on the QFR (quartz-feldspar-rock fragments) ternary diagram of Folk (1980) and Pettijohn (1975). Triangular classification diagram indicates that the sandstones are quartz arenite to sublitharenite (Fig. 6).

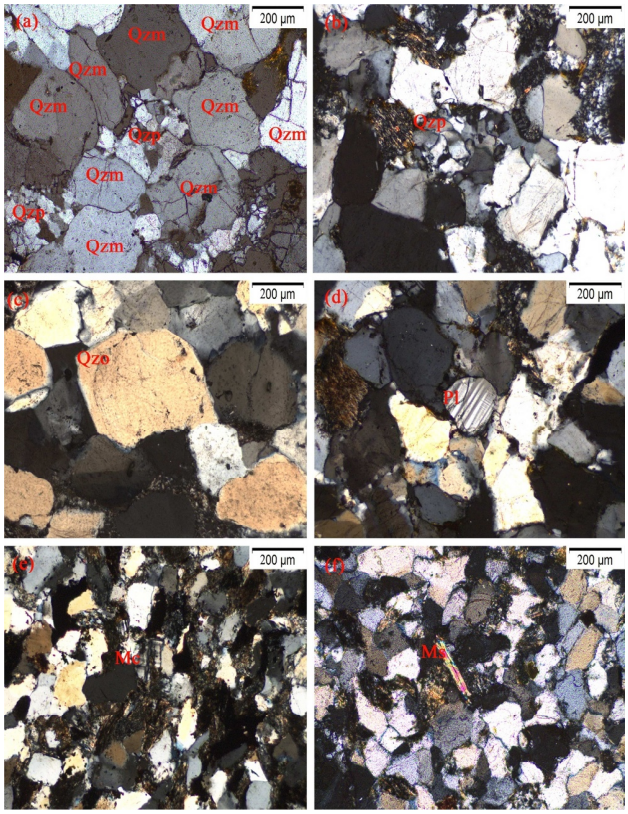

Fig.4. Photomicrographs of the Kopili sandstones: (a) Monocrystalline (Qzm) and polycrystalline quartz (Qzp), (b) Polycrystalline quartz (Qzp), (c) Quartz overgrowth (Qzo), (d) Plagioclase feldspar (Pl), (e) Microcline (Mc), (f) Muscovite (Ms).

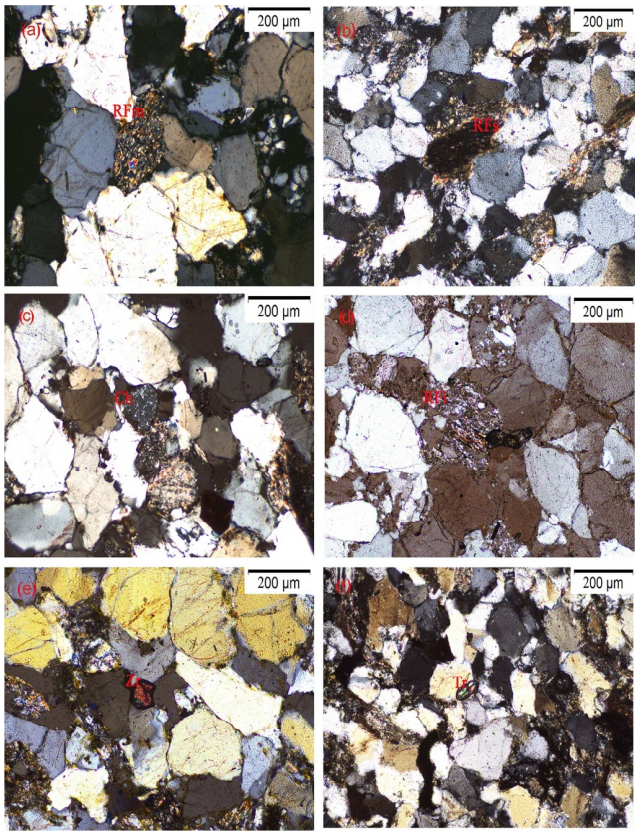

Fig. 5. Photomicrographs of the Kopili sandstones: (a) Metamorphic rock fragment (Rfm), (b) Sedimentary rock fragment (Rfs), (c) Chert (Ch), (d) Igneous rock fragment (Rfi), (e) Zircon (Zrn) and (f) Tourmaline (Tur).

Table 2. Results of petrographic modal analysis of the Kopili Formation sandstone (in volume % of rocks)

Sample	Qm	Qp	Qt	Pl	Mi	F	Cement	Matrix	R	Mu	Bi	Mica	Mis
1F	58.6	26.56	85.16	0.34	0.25	0.59	2.2	1.78	4.6	3.62	1.8	5.42	0.25
2F	57.06	26.26	83.32	0.23	0.23	0.46	1.86	1.96	6.49	5.6	0	5.6	0.31
3F	52.08	26.54	78.62	0.31	0.08	0.39	3.96	4.45	7.01	3.61	1.7	5.31	0.26
4F	57.25	29.59	86.84	0.8	0.36	1.16	3.46	2.92	3.82	1.22	0	1.22	0.58
5F	54.96	26.83	81.79	0.46	0	0.46	3.11	1.86	4.85	6.33	0.9	7.23	0.7
6F	50.52	28.18	77.7	0.56	0	0.56	3.36	3.33	9.81	4.68	0	4.68	0.56
7F	57.12	28.65	85.77	0.55	0.18	0.73	4.21	1.82	4.46	2.28	0	2.28	0.73
8F	53.91	34.37	88.28	0.76	0.38	1.14	4.73	1.89	2.07	1.06	0.26	1.32	0.57
9F	52.91	22.65	75.56	0.18	0	1.18	2.41	7.78	11.48	0.88	0	0.88	0.71
10F	50.16	26.83	76.99	0.71	0	0.71	8.53	1.53	10.06	1.82	0.36	2.18	0
11F	55.54	33.73	89.27	0.16	0.16	0.33	4.28	2.63	2	1.33	0	1.33	0.16
12F	54.5	33.07	87.57	0.49	0	0.49	3.61	2.43	2.77	3.1	0	3.1	0
13F	54.34	30.87	85.21	0.18	0.35	0.53	4.4	3.69	2.11	4.06	0	4.06	0
14F	56.62	32.92	89.54	0.31	0.15	0.46	2.23	1	3	3.77	0	3.77	0
15F	57.96	27.97	85.93	0.33	0	0.33	4.97	4.12	2.99	1.66	0	1.66	0
17F	50.52	29.7	80.22	0	0.16	0.16	5.8	4.42	4.12	4.55	0.57	5.12	0
19F	54.59	29.97	84.56	0.18	0	0.18	4.97	4.73	3.81	1.4	0	1.4	0.35
20F	56.52	28.83	85.35	0.18	0.18	0.36	2.04	2.48	7.56	1.65	0	1.65	0.55
21F	49.06	26.46	75.52	0.38	0	0.38	7.47	6.45	7.52	7.09	0	7.09	0.57
22F	53.84	26.23	80.07	0.18	0	0.18	7.02	5.27	3.93	4.36	2.8	7.16	0.37
23F	58.09	29.14	87.23	0.54	0	0.54	2.89	2.96	4.98	1.73	0.29	2.02	0.54
24F	62.72	27.31	90.03	0.37	0	0.37	4.8	2.59	1.48	0.55	0	0.55	0.18
25F	57.77	32.7	90.47	0	0	0	2.08	1.56	2.92	2.23	0.74	2.97	0
26F	49.79	25.44	75.23	0	0.19	0.19	6.67	3.99	6.44	6.57	0.72	7.29	0.19
27F	52.62	31.83	84.45	0	0	0	4.59	1.92	6.45	2.4	0	2.4	0.19
28F	52.38	30.67	83.05	0.19	0	0.19	3.09	4.28	4.9	3.49	0	3.49	0
29F	62.06	20.59	80.65	0.5	0.11	0.61	2.64	3.86	9.47	5.35	0	5.35	0.51
31F	54.57	27.58	82.15	0.32	0	0.32	2.11	4.67	7.97	2.78	0	2.78	0
15.2R	58.31	20.24	78.55	0.18	0	0.18	4.26	5.01	7.56	3.23	0.64	3.87	0.57
49D	57.97	20.29	78.26	0.38	0	0.38	3.54	5.09	8.06	3.74	0.74	4.48	0.19
22D	56.03	20.56	76.59	0.65	0	0.65	7.81	4.3	6.78	3.25	0	3.25	0.62
37D	53.4	17.2	70.6	0.31	0.09	0.4	6.9	8.1	10.2	2.2	0	2.2	0.2
42D	51.4	21	72.4	0.72	0.08	0.8	4.4	4.2	15.2	1.2	0	1.2	0
38D	50.1	19.1	69.2	0	0	0	2.2	7.2	19.6	1.6	0	1.6	0.2
Avg.	54.86	27.05	81.83	0.34	0.09	0.45	4.19	3.71	6.37	3.07	0.34	3.41	0.3
Min	49.06	17.2	69.2	0	0	0	1.86	1	1.48	0.88	0	0.55	0
Max	62.06	34.37	90.47	0.76	0.38	1.18	8.53	8.1	19.6	7.09	0.74	7.29	0.73

Qm= Monocrystalline quartz, Qp= Polycrystalline quartz, Qt= Total qrtz, Pl= Plagioclage, Mi= Microcline, F= Total Feldspar, R= Rock fragments, Mu= Muscovite, Bi= Biotite, Mis= Miscellaneous

GEOCHEMISTRY

The Kopili sandstones are characterized with the high content of SiO_2 (72.67 - 96.99 wt %, avg. 86.28 wt%) followed by low content of Al_2O_3 (1.38 - 13.96 wt%, avg. 5.72 wt%), TiO_2 (0.18 - 1.03 wt%, avg. 0.54 wt%), Fe_2O_3 (0.58 - 7.11 wt%, avg. 2.50 wt%), MgO (0.06 - 1.33 wt%, avg. 0.49 wt%), CaO (0.06 - 0.52 wt%, avg. 0.25 wt%), Na_2O (0.26-1.20 wt%, avg. 0.55 wt%), K_2O (0.38 - 2.20 wt%, avg. 1.09 wt%) and P_2O_5 (0.02 - 0.29 wt%, avg. 0.11 wt%) (Table 3). The higher content of SiO_2, in comparison to the other major oxides, classifies these sandstones as quartz rich to quartz-arenite type (76-95wt%; Condie, 1993). The SiO_2/Al_2O_3 (avg. 21.90 wt%) ratio indicates highly mature nature of the Kopili sandstones. These sandstones have higher SiO_2/Al_2O_3 ratio than upper continental crust (UCC, SiO_2/Al_2O_3=4.38; Condie, 1993). The concentration of CaO, Na_2O, K_2O, and K_2O/Na_2O ratio indicate dominance of K - feldspar as compared to the plagioclase (Table 3). Major element geochemical classification diagram of Pettijohn et al. (1972) classifies these sandstones as arkose to sub-litharenite type (Fig. 7).

The Kopili sandstones are characterised by high content of large ion lithophile elements (LILE) like Ba (105.14 - 274.17, avg. 152.13), Rb (26.80 - 76.53, avg. 39.80), Sr (29.93 - 63.34, avg. 40.98), Cs (1.17 - 3.06, avg. 1.65), Th (8.09 - 21.51, avg. 13.77) and U (1.03 - 3.48, avg. 1.80) (Table 4). The strong positive correlation of K_2O with Rb (r=0.67), Sr (r=0.63), Ba (r=0.67), Th (r=0.44), U (r=0.57), and Cs (r=0.67) indicate that the LILEs are mostly controlled by alkali feldspar and clay minerals. In terms of transition trace elements (TTEs), the Kopili sandstones have high content of Sc (4.67 - 10.29, avg. 6.93), V (35.43 - 85.82, avg. 55.27), Cr (24.68 - 83.80, avg. 42.82) Co (3.14 - 9.90, avg. 6.53), and Ni (13.50 - 19.22, avg. 16.38) (Table 4). During weathering the TTEs are mostly accommodated in the clay bearing minerals. Al_2O_3 shows positive correlation with Sc (r=0.55), V (r=0.62), Cr (r=0.62), Co (r=0.44) and Ni (r=0.44) suggesting control of the clay-bearing minerals on the TTEs of the Kopili sandstones.

High field strength elements (HFSEs) are preferentially partitioned into melts during crystallization and anatexis (Feng and Kerrich, 1990), and as a result, these elements are enriched in felsic rather than mafic igneous rocks. Additionally, along with the REEs, they reflect provenance compositions as a consequence of their immobile behaviour (Taylor and McLennan, 1985). The Kopili sandstones are characterised by moderate to enriched concentration of the HFSEs (Zr=132.47 - 731.57, avg. 343.81; Hf=4.05 - 22.40, avg. 10.58; Nb=6.90 - 20.29, avg. 11.16; and Y=13.34 - 34.54, avg. 19.78) (Table 4).

REEs are not easily fractionated during sedimentation, sedimentary REE patterns may provide an index to average provenance compositions (McLenan, 1989). The chondrite normalised (Sun and McDonough, 1989) REE patterns of the Kopili sandstones show LREE

Table 3. Major element composition of the Kopili Formation sandstone. Major oxides are in wt%.

Sample	5F	6F	8F	9F	10F	11F	12F	15F	17F	19F	21F	22F	24F	22D	37D	38D	42D	49D	15.2R	Avg.	Min.	Max.
SiO_2	83.51	84.81	94.11	86.31	96.99	94.65	92.20	88.96	94.03	92.98	72.67	72.91	83.85	84.07	82.49	80.01	82.78	86.81	85.23	86.28	72.67	96.99
Al_2O_3	5.90	5.85	2.40	7.14	1.38	2.10	3.31	4.79	3.08	3.25	11.78	13.96	6.99	6.89	5.91	9.90	4.74	3.32	6.08	5.72	1.38	13.96
Fe_2O_3	4.82	2.49	1.20	2.48	0.58	1.06	1.12	1.88	1.08	1.34	7.11	3.82	3.12	3.10	3.99	2.64	2.27	0.68	2.64	2.50	0.58	7.11
MnO	0.01	0.02	0.01	0.01	0.01	0.01	0.01	0.02	0.01	0.02	0.04	0.02	0.02	0.02	0.02	0.02	0.14	0.01	0.01	0.02	0.01	0.14
MgO	0.29	0.29	0.23	0.32	0.10	0.21	0.25	0.22	0.14	0.20	1.17	0.80	0.38	1.08	1.03	1.02	1.33	0.06	0.25	0.49	0.06	1.33
CaO	0.24	0.31	0.20	0.17	0.06	0.19	0.21	0.23	0.11	0.21	0.26	0.22	0.31	0.52	0.48	0.35	0.20	0.42	0.08	0.25	0.06	0.52
Na_2O	0.30	0.48	0.40	0.36	0.27	0.26	0.41	0.52	0.35	0.46	0.74	0.73	0.50	0.86	1.20	0.80	0.58	0.87	0.45	0.55	0.26	1.20
K_2O	1.01	0.84	0.76	1.03	0.38	0.53	0.62	0.74	0.65	0.71	1.40	2.20	0.84	1.18	1.48	1.53	1.30	2.19	1.23	1.09	0.38	2.20
TiO_2	0.57	0.46	0.34	0.65	0.18	0.38	0.47	0.45	0.21	0.43	0.85	1.03	0.66	0.99	0.73	0.41	0.70	0.44	0.32	0.54	0.18	1.03
P_2O_5	0.18	0.08	0.03	0.07	0.02	0.05	0.07	0.07	0.06	0.05	0.16	0.11	0.09	0.17	0.16	0.13	0.14	0.11	0.29	0.11	0.02	0.29
LOI	2.69	3.59	0.30	2.18	0.02	0.46	1.06	1.29	0.25	0.30	3.78	3.00	1.90	1.09	1.20	1.50	1.80	3.10	1.45	1.63	0.02	3.78
Na_2O/K_2O	0.30	0.57	0.53	0.35	0.71	0.49	0.66	0.70	0.54	0.65	0.53	0.33	0.60	0.73	0.81	0.52	0.45	0.40	0.37	0.54	0.30	0.81
Sio_2/Al_2O_3	14.15	14.50	39.21	12.09	70.28	45.07	27.85	18.57	30.53	28.61	6.17	5.22	12.00	12.20	13.96	8.08	17.46	26.15	14.02	21.90	5.22	70.28
Fe_2O_3/K_2O	4.77	2.96	1.58	2.41	1.53	2.00	1.81	2.54	1.66	1.89	5.08	1.74	3.71	2.63	2.70	1.73	1.75	0.31	2.15	2.36	0.31	5.08
K_2O/Al_2O_3	0.17	0.14	0.32	0.14	0.28	0.25	0.19	0.15	0.21	0.22	0.12	0.16	0.12	0.17	0.25	0.15	0.27	0.66	0.20	0.22	0.12	0.66
TiO_2/Al_2O_3	0.10	0.08	0.14	0.09	0.13	0.18	0.14	0.09	0.07	0.13	0.07	0.07	0.09	0.14	0.12	0.04	0.15	0.13	0.05	0.11	0.04	0.18
Fe_2O_3/Al_2O_3	0.82	0.43	0.50	0.35	0.42	0.50	0.34	0.39	0.35	0.41	0.60	0.27	0.45	0.45	0.68	0.27	0.48	0.20	0.43	0.44	0.20	0.82
Al_2O_3/TiO_2	10.35	12.72	7.06	10.98	7.67	5.53	7.04	10.64	14.67	7.56	13.86	13.55	10.59	6.96	8.10	24.15	6.77	7.55	19.00	10.78	5.53	24.15
K_2O/Na_2O	3.37	1.75	1.90	2.86	1.41	2.04	1.51	1.42	1.86	1.54	1.89	3.01	1.68	1.37	1.23	1.91	2.24	2.52	2.73	2.01	1.23	3.37
CIA	74.43	72.08	56.51	77.95	58.83	60.89	65.68	69.75	67.52	62.99	78.58	77.78	75.25	65.42	57.02	73.26	63.46	42.06	73.25	66.98	42.06	78.58
CIW	86.37	81.20	70.13	88.78	71.37	73.07	75.80	78.99	79.87	74.04	87.45	89.71	83.44	74.47	67.48	83.52	78.24	60.19	87.28	78.49	60.19	89.71
PIA	83.77	78.48	60.64	86.97	63.61	66.34	71.39	75.78	75.37	68.52	85.85	87.84	81.42	70.37	60.18	80.83	71.63	30.05	84.27	72.81	30.05	87.84
ICV	0.24	0.20	0.37	0.20	0.31	0.30	0.23	0.20	0.25	0.27	0.23	0.24	0.18	0.27	0.36	0.23	0.37	0.75	0.26	0.29	0.18	0.75

Table 4. Trace element and REE composition of the Kopili Formation sandstone. The concentrations of trace elements in ppm. Eu/Eu*: EuN/(SmN × GdN)$^{1/2}$. REE normalizing values are from after (Sun and McDonough, 1989).

Sample no	5F	6F	8F	9F	10F	11F	12F	14F	15F	17F	19F	22F	24F	37D	42D	Avg.	Min.	Max.
Sc	6.22	6.07	7.08	7.94	7.00	6.45	7.63	5.88	4.96	8.55	4.67	10.29	6.81	7.91	6.49	6.93	4.67	10.29
V	53.25	51.98	52.61	62.05	52.30	50.02	61.91	46.13	37.99	70.05	35.43	85.82	54.27	62.71	52.51	55.27	35.43	85.82
Cr	33.80	31.53	32.66	58.21	32.10	43.77	56.56	31.85	29.32	59.09	24.68	83.80	34.38	53.22	37.32	42.82	24.68	83.80
Co	3.14	6.89	5.01	5.96	5.95	6.14	8.10	6.50	6.31	8.30	6.38	9.90	6.70	7.33	5.32	6.53	3.14	9.90
Ni	13.50	17.74	15.62	18.18	16.68	16.47	16.99	15.27	14.76	17.50	15.31	19.22	15.77	17.46	15.25	16.38	13.50	19.22
Cu	18.25	26.61	22.43	16.79	24.52	17.67	20.40	18.46	18.54	20.31	18.98	22.25	18.38	21.48	18.10	20.21	16.79	26.61
Zn	35.35	118.87	77.11	45.78	97.99	51.01	190.58	49.29	56.24	183.63	38.26	324.92	42.33	157.98	42.90	100.82	35.35	324.92
Ga	7.55	7.01	7.28	9.44	7.15	7.73	9.68	6.67	6.02	10.33	5.87	13.35	7.32	9.41	7.53	8.16	5.87	13.35
Rb	38.11	33.66	35.88	40.85	34.77	33.82	51.66	29.04	26.80	53.90	27.95	76.53	31.28	48.37	34.41	39.80	26.80	76.53
Sr	39.25	39.66	39.45	41.13	39.55	35.53	46.64	31.81	29.93	48.52	43.96	63.34	33.69	46.14	36.16	40.98	29.93	63.34
Y	13.61	13.34	13.47	26.10	13.41	21.53	25.75	16.67	16.96	25.46	19.17	34.54	16.38	23.16	17.18	19.78	13.34	34.54
Zr	204.95	132.47	168.71	689.83	150.59	442.31	463.18	237.69	194.78	506.08	203.57	731.57	280.59	441.49	309.28	343.81	132.47	731.57
Nb	9.67	7.65	8.66	12.85	8.16	10.40	14.12	9.77	7.95	15.94	6.90	20.29	11.59	12.95	10.55	11.16	6.90	20.29
Cs	1.58	1.39	1.48	1.68	1.43	1.42	2.11	1.19	1.17	2.13	1.50	3.06	1.21	1.97	1.41	1.65	1.17	3.06
Ba	144.42	131.79	138.10	155.55	134.94	130.35	189.65	115.28	105.14	199.79	124.10	274.17	125.41	179.82	133.39	152.13	105.14	274.17
Hf	6.43	4.05	5.24	21.23	4.64	13.58	14.17	7.37	5.94	15.60	6.16	22.40	8.81	13.54	9.61	10.58	4.05	22.40
Ta	1.07	0.23	0.65	0.61	0.44	0.59	1.38	0.59	0.57	1.40	0.50	2.18	0.61	1.07	0.76	0.84	0.23	2.18
Pb	12.93	23.22	18.07	50.00	20.64	33.66	21.56	15.11	17.33	19.35	12.50	25.79	12.90	26.70	19.83	21.97	12.50	50.00
Th	9.50	8.09	8.79	21.51	8.44	17.76	17.69	12.63	14.02	16.30	10.49	21.36	11.25	15.85	12.84	13.77	8.09	21.51
U	1.20	1.03	1.11	2.70	1.07	2.03	2.42	1.37	1.36	2.43	1.73	3.48	1.38	2.19	1.54	1.80	1.03	3.48
La	27.86	27.24	27.55	49.36	27.39	39.53	39.62	28.80	29.70	38.71	25.29	49.54	27.89	38.82	31.76	33.94	25.29	49.54
Ce	57.97	57.63	57.80	105.22	57.72	83.99	81.33	59.61	62.75	78.18	55.22	99.90	56.46	80.54	66.14	70.70	55.22	105.22
Pr	7.03	7.00	7.01	12.63	7.00	10.09	9.62	7.20	7.55	9.26	6.44	11.68	6.84	9.59	7.99	8.46	6.44	12.63
Nd	26.22	26.91	26.22	46.97	26.56	37.43	35.31	27.03	27.89	34.45	24.48	42.74	26.17	35.58	29.94	31.59	24.48	46.97
Sm	4.91	5.09	5.00	8.59	5.04	6.87	6.36	5.10	5.14	6.32	4.85	7.58	5.05	6.50	5.61	5.87	4.85	8.59
Eu	0.95	0.98	0.96	1.36	0.97	1.11	1.12	0.95	0.86	1.21	0.94	1.37	1.05	1.15	1.03	1.07	0.86	1.37
Gd	3.40	3.76	3.58	6.18	3.67	5.16	5.21	4.09	4.15	5.16	4.33	6.27	4.04	5.03	4.20	4.55	3.40	6.27
Tb	0.54	0.57	0.55	0.99	0.56	0.83	0.89	0.67	0.68	0.89	0.73	1.10	0.67	0.83	0.68	0.75	0.54	1.10
Dy	2.60	2.74	2.67	4.96	2.70	4.15	4.75	3.30	3.34	4.72	3.67	6.17	3.27	4.34	3.34	3.78	2.60	6.17
Ho	0.50	0.50	0.70	0.95	0.60	0.79	0.95	0.63	0.63	0.95	0.69	1.26	0.63	0.88	0.64	0.75	0.50	1.26
Er	1.40	1.34	1.37	2.72	1.35	2.21	2.69	1.71	1.70	2.70	1.85	3.68	1.72	2.41	1.78	2.04	1.34	3.68
Tm	0.22	0.21	0.21	0.45	0.21	0.36	0.44	0.27	0.27	0.44	0.29	0.62	0.26	0.40	0.28	0.33	0.21	0.62
Yb	1.46	1.34	1.40	3.01	1.37	2.33	2.87	1.67	1.65	2.90	1.77	4.10	1.70	2.60	1.83	2.13	1.34	4.10
Lu	0.22	0.21	0.21	0.47	0.21	0.37	0.45	0.27	0.26	0.46	0.28	0.65	0.28	0.41	0.29	0.34	0.21	0.65
ΣLREE	128.34	128.60	128.12	230.31	128.36	184.18	178.55	132.77	138.04	173.28	121.55	219.07	127.50	177.20	146.67	156.17	121.55	230.31
ΣHREE	6.94	6.91	7.11	13.57	7.01	11.04	13.05	8.52	8.51	13.06	9.28	17.59	8.52	11.88	8.83	10.12	6.91	17.59
LREE/HREE	18.50	18.61	18.02	16.98	18.31	16.69	13.68	15.59	16.22	13.27	13.10	12.45	14.96	14.92	16.60	15.86	12.45	18.61
Eu/Eu*	0.71	0.68	0.69	0.57	0.69	0.57	0.59	0.64	0.57	0.65	0.63	0.61	0.71	0.61	0.65	0.64	0.57	0.71
(La/Sm)N	3.66	3.45	3.56	3.71	3.51	3.71	4.02	3.65	3.73	3.95	3.37	4.22	3.57	3.86	3.65	3.71	3.37	4.22
(Gd/Yb)N	1.93	2.32	2.12	1.70	2.22	1.83	1.50	2.03	2.08	1.47	2.02	1.27	1.97	1.60	1.90	1.86	1.27	2.32
(La/Yb)N	13.69	14.58	14.12	11.76	14.34	12.17	9.90	12.37	12.91	9.57	10.25	8.67	11.77	10.71	12.45	11.95	8.67	14.58

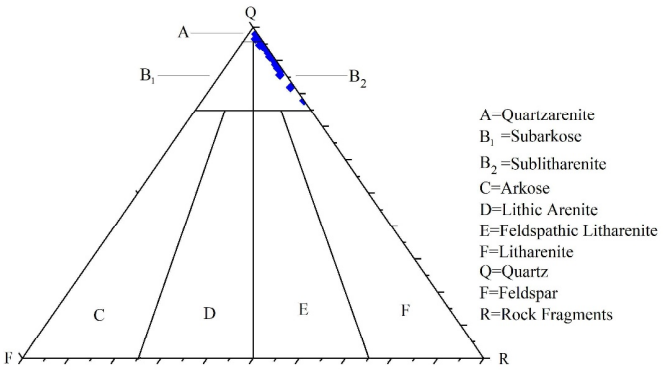

Fig. 6. Triangular classification Plots of Kopili sandstones (after Folk, 1980).

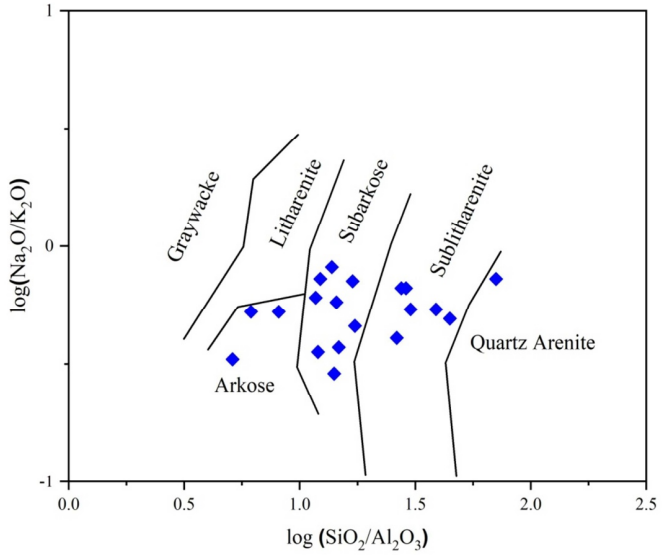

Fig. 7. Bivariate plot of log (Na_2O/K_2O) vs. log (SiO_2/Al_2O_3) of Kopili sandstones (Pettijohn et al., 1972).

enrichment (La/SmN=3.37 - 4.22, avg. 3.71) and HREE depletion (Gd/YbN=1.27 - 2.32, avg. 1.86) coupled with negative Eu anomaly (Eu/Eu*=0.57 - 0.71, avg. 0.64) (Table 4; Fig. 8). The strong positive correlation of ΣREE with Al_2O_3 (r= 0.50) and Zr (r= 0.97) and negative correlation with SiO_2 (r= -0.34) are related with the quartz dilution effect. The positive correlation of ΣREE is also observed with K_2O, TiO_2, and Nb that indicate REEs are controlled by clay bearing minerals, zircon and rutile.

In UCC normalised (Taylor and McLennan, 1985) multi-element spider diagram, the sandstones are mostly found depleted in all major oxides (except SiO_2 and TiO_2). Depletion of LILE like Rb, Sr, and Ba (except Th and U) and TTEs is also observed while REEs are showing nearly similar pattern with UCC (Fig. 9). Based on these interpretations it is suggested that the Kopili sandstones are basically derived from the upper continental crust and the depletion and enrichment is related to the variable rate of chemical weathering.

HYDRAULIC SORTING

Sedimentary processes like hydraulic sorting (grain size effect) may significantly modify the mineral abundances and consequently the concentrations of many elements. Clay minerals which are major hosts of many elements are preferentially accumulated in the finer fraction during hydrological/sedimentary processes. In the following discussion, we evaluate the sorting effect by synthesizing geochemical composition of the Kopili sandstones. The detrital modes of the Kopili sandstones suggest more mature nature which is further corroborated

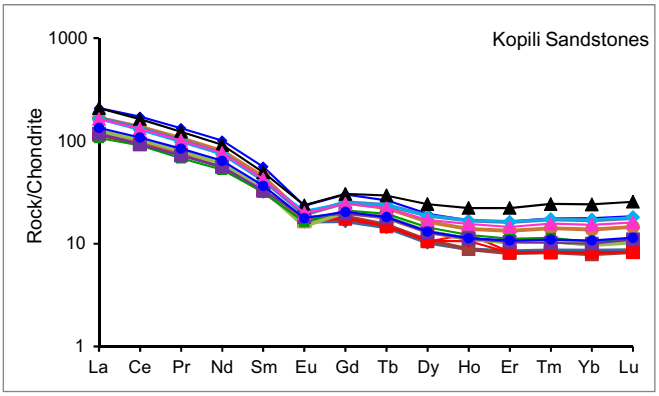

Fig. 8. Chondrite normalised REE patterns of the Kopili sandstones (Sun and McDonough, 1989).

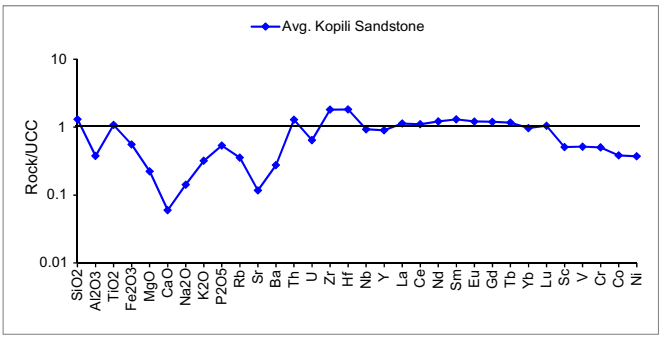

Fig. 9. UCC normalized multielement pattern in Kopili sandstones (Taylor and McLennan 1985).

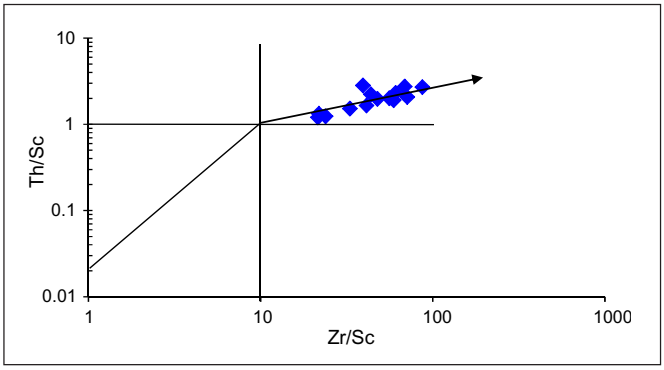

Fig. 10. Th/Sc versus Zr/Sc plot of Kopili Formation sandstones (after McLennan et al., 1993).

by their mean SiO_2/Al_2O_3 ratio (avg. 21.90). If it is due to the quartz dilution effect, then studied sandstones should contain lower concentrations of ΣREE. However, it is opposite which may occur due to fractionation of heavy minerals (i.e., zircon, monazite, apatite, sphene, and allanite) and feldspars through hydraulic sorting. The Th/Sc versus Zr/Sc diagram (McLennan et al., 1993) (Fig. 10) is considered a better tool to constrain the sorting effect on clastic sedimentary rocks. In this diagram samples plotting to the right of the composition line are considered to be enriched in zircon (McLennan et al. 1993). The Kopili sandstone samples in this diagram plot exclusively on zircon enrichment trend line with minor sorting effect.

DISCUSSION

Paleo-weathering

The intensity of chemical weathering in source area plays an

important role to change the mineralogical as well as chemical composition of the clastic rocks (Nesbitt et al., 1996). Various weathering indices like Chemical Index of Alteration (CIA= [Al_2O_3/ (Al_2O_3 + CaO* + Na_2O + K_2O)] *100), Chemical Index of Weathering (CIW= [Al_2O_3/ (Al_2O_3 + CaO* + Na_2O)] *100), Plagioclase Index of Alteration (PIA= [(Al_2O_3 - K_2O)/ (Al_2O_3 + CaO* + Na_2O - K_2O)] *100), and A - CN - K ternary diagram are useful to decipher the intensity of chemical weathering (Nesbitt and Young, 1984, 1989, Fatima and Khan, 2012; Khan and Khan, 2015, 2016; Absar et al., 2016; Khan et al., 2019, 2020). The CIA calculation has been done with the formula of Nesbitt et al. (1996), and CaO* represents CaO in silicate fractions. The range and average of the CIA and CIW (Table 3), suggest mostly low to moderate degree of chemical weathering (except 49D sample) for the Kopili sandstones. The intensity of the chemical weathering can also be estimated using the Plagioclase Index of Alteration (PIA). Unweathered plagioclase has a PIA value of 50. The PIA values for the studied samples (Table 3), also justify the above observation.

The A - CN - K ternary diagram is also useful to identify the provenance composition and weathering trend (Nesbitt and Young, 1984; Fedo et al., 1995). Weathering leads to removal of CaO, Na_2O and K_2O and the weathering trend moves parallel to the A - CN and A - K line that depends upon the intensity of leaching of CaO, Na_2O and K_2O. Majority of the samples in A - CN - K ternary diagram (Fig. 11) are plotted on 2 to 5 weathering trend line which indicate low to moderate degree of chemical weathering in arid to semi-humid climatic conditions. The SiO_2 versus (Al_2O_3 + K_2O + Na_2O) diagram (Fig. 12) discriminates between humid and arid climates and, show degree of chemical maturity (Suttner and Dutta, 1986). The plotting pattern of the Kopili sandstone samples in this diagram indicates humid climatic condition and high degree of chemical maturity.

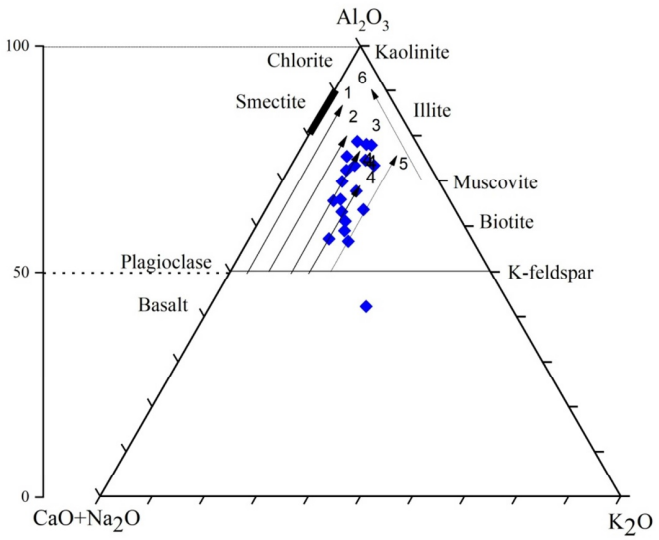

Fig. 11. Ternary plot of A-CN-K for Kopili sandstones (after Nesbitt and Young, 1984). Arrows 1 to 6 express compositional trend of initial weathering profile of various rock types, 1-Gabbro, 2-Tonalite, 3-diorite, 4-granodiorite, 5-granite, and 6-advance weathering trend.

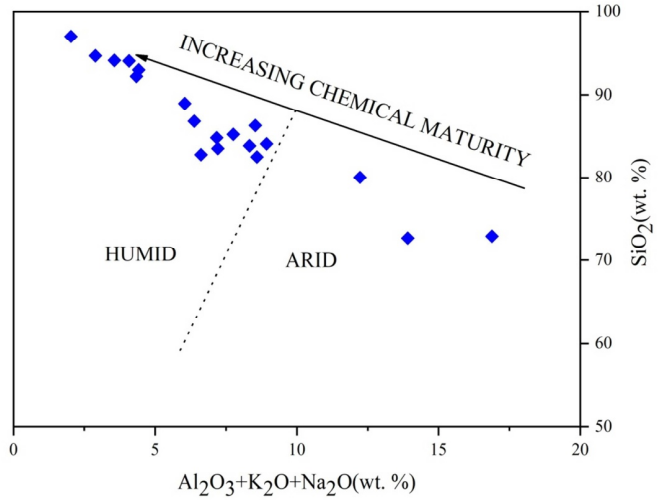

Fig. 12. Plot of Al_2O_3 + K_2O + Na_2O versus SiO_2 of Kopili sandstones (after Suttner and Dutta, 1986).

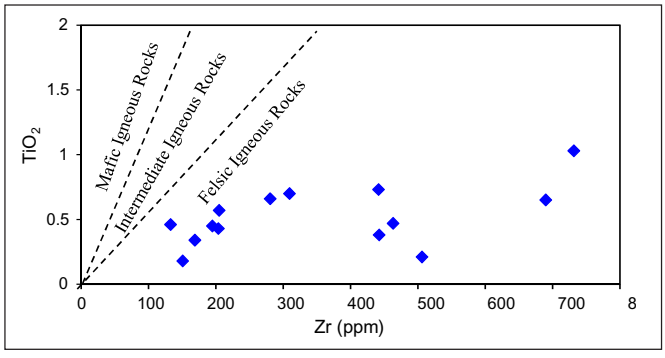

Fig. 13. The TiO_2 versus Zr binary diagram for the Kopili sandstones.

Provenance

The chemical composition of sedimentary rocks is controlled by a complex set of parameters namely erosion, transport and deposition. The principal first-order parameters include source rock composition, modification by chemical weathering, mechanical disaggregation and abrasion, authigenic inputs, hydraulic sorting, and diagenesis (Johnsson, 1993; Walsh et al., 2016). For example, alkali and alkaline earth elements, such as K, Na, Ca and Sr may be transported as dissolved species and their abundances in sedimentary rocks may not reflect their abundances in source terrain (Sheldon et al., 2002). The petrographic modes, A - CN - K ternary diagram, immobile elements and their ratios (including REEs) are helpful in identification of the provenance or source rock characteristics. Variable range of Al_2O_3/ TiO_2 ratio occurs in mafic igneous rocks (3 - 8), intermediate igneous rocks (8 - 21) and felsic igneous rocks (21 - 70) (Hayashi et al., 1997). The range and average of Al_2O_3 / TiO_2 ratio of the Kopili sandstone (5.53 - 24.15, avg. 10.78) (Table 3) suggests intermediate igneous rock type provenance. The TiO_2 versus Zr binary diagram (Fig. 13) also indicate felsic dominant source rocks for the Kopili sandstones (Hayashi et al., 1997). The plot of CIA verses ICV weathering indices has been used to interpret the source rock characteristics (Potter et al., 2005) (Fig. 14). The fields in this diagram are based on the weathering trends of the most abundant crustal igneous rocks i.e., basalt, granite and andesite. The Kopili sandstones are mostly plotted in the granite trend line field, which suggests their derivation from granitic source rocks. The major element-based discrimination diagram of Roser and Korsch (1988) is also useful to decipher the source rock characteristics. The plotting pattern in this diagram supports the above observation (Fig. 15).

The ratios of Th/Sc and Zr/ Sc indicates compositional variation in mineral, sorting extent and content of heavy mineral in sediments (McLennan et al., 1993). Plot of Th/Sc versus Zr/Sc (Fig. 10) reflects derivation of Kopili sandstones from granitic (felsic) source and the recycled sediments. Enrichment of Zr may be because of the composition of the source and interchange of hydraulic sorting.

The REE pattern with their ratios and magnitude of Eu anomaly is also useful to decipher the provenance of the sedimentary rocks

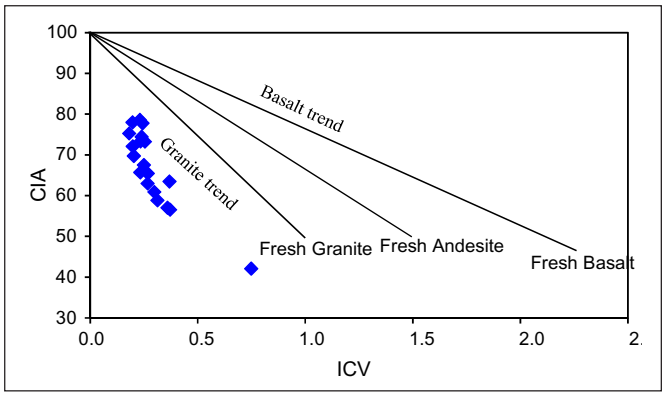

Fig. 14. Chemical Index of Alteration (CIA) versus Index of Chemical Variation (ICV) plot for the Kopili sandstones (Potter et al., 2005).

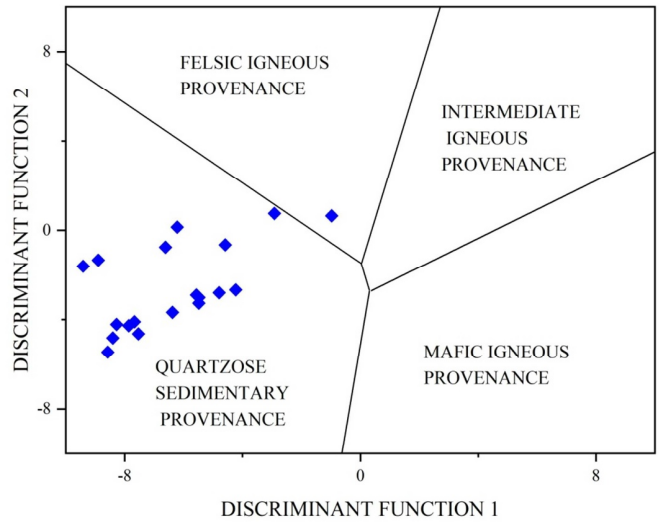

Fig.15. Discriminant function diagram for the Kopili sandstones (Roser and Korsch, 1988); Discriminant function 1= (-1.773 TiO_2)+ (0.607Al_2O_3)+ (0.760 Fe_2O_3)+ (1.500 MgO) + (0.616 CaO)+ (0.509Na_2O)+(-1.224 K_2O)+ (-9.090); Discriminant function 2=(0.445TiO_2)+ (0.070 Al_2O_3)+ (-0.250 Fe_2O_3)+ (-1.142 MgO)+(0.438 CaO)+ (1.475 Na_2O)+ (-1.426 K_2O)+ (-6.861).

(McLennan et al., 1990). The Kopili sandstones are characterized by enriched LREE pattern (La/SmN =3.37 - 4.22, avg. 3.71) with flat or depleted HREE pattern (Gd/YbN =1.27 - 2.32, avg. 1.86) and negative Eu anomaly (0.57 - 0.71, avg. 0.64). The felsic igneous rocks have high La/YbN ratio and negative Eu anomaly while mafic igneous rocks are characterized with low La/YbN ratio with positive or nearly positive Eu anomaly (McLennan et al., 1990). Various trace element ratios of the Kopili sandstones are compared with coarse grained felsic and mafic source rocks of Cullers (2000) and, Cullers and Podkovyrov (2000) (Table 5). It indicates that the Kopili sandstones are mostly felsic in nature with minor contribution of mafic source rocks.

Based on the source rock composition it has been suggested that sandstones of Kopili Formation received sediments from felsic dominant source with small contribution from mafic source rocks. The most probable source may be the Shillong Plateau granites and basalts. The generalized paleocurrent directions from north to south of the studied formation also indicate Shillong Plateau as the main source for the Kopili sandstones. In order to identify the source rock components, the chondrite normalized REE based provenance modelling is considered a valuable tool (e.g., Hofmann, 2005; Roddaz et al., 2007). In this provenance modelling it is necessary that mass balance should be taken into consideration. It is known that pelitic

Table 5. Range of elemental ratios in sandstone samples of the Kopili Formation compared with the range of ratios in similar fractions derived from felsic and basic rocks. (Standard's data source Cullers, 2000; Cullers and Podkovyrov, 2002), and Upper Continental Crust (UCC) (Condie, 2003).

Elemental ratios	Coarse Fraction		UCC	Kopili Sandstone
	Range of sediments from			
	Felsic sources	Basic sources		
Eu/Eu*	0.40–0.94	0.71–0.95	0.76	0.57–0.71
La/Sc	2.5–16.3	0.43–0.86	2.21	3.89–6.22
Th/Sc	0.84–20.5	0.05–0.22	0.79	1.21–2.83
La/Co	1.8–13.8	0.14–0.38	1.76	3.95–8.87
Th/Co	0.67–19.4	0.04–1.4	0.63	1.17–3.61
Cr/Th	4.0-15.0	25-500	7.76	2.09–3.92
$(La/Lu)_N$	3.0-27.0	1.10-17.0	9.73	8.17–14.06

rocks (shale) and sandstones include 70 and 30%, respectively of the total mass of sediments (Mackenzie and Garrels, 1971; Taylor and McLennan, 1985), consequently a mixture of 70% shale and 30% sandstone is taken as model composition, but because of unavailability of the shale data only sandstone REE data has been utilized. As probable source rocks, Sylhet Trap Basalts (STB) from Shillong plateau (Hussain et al., 2020), Mylliem Granitoids (MG) (Ray et al., 2011) and Diorite (D) around Umsopri of Ri-bhoi district (Gogoi and Bhagabaty, 2018) have been selected for provenance modeling. Based on REE provenance modeling it has been found that Kopili sandstones received sediments in the proportion of 0.1% STB: 0.5 % MG: 0.4 % D. The further authentication of this proportion can be done by dating detrital zircon grains.

Tectonic Setting

Triangular plot of Qm-F-Rt (after Dickinson and Suczek, 1979) depicts that Kopili sandstone were originated from recycled orogen (Fig. 16). The chemical composition of the clastic mostly depends on the source area characteristics and their geological setting (Bhatia, 1983; Bhatia and Crook, 1986). Roser and Korsch (1986) have developed tectonic discrimination diagram based on major element geochemistry (Fig. 17). The majority of the samples in this diagram are plotted in the passive margin field indicating derivation of the sediments from adjoining stable continental or rifted margin. Various plots have been proposed to determine tectonic settings using some particular trace elements like Th, La, Y, Sc, Cr, Co and Zr rather than major elements as these trace elements are more stable than major elements under depositional condition (Bhatia and Crook, 1986; Roser and Korsch, 1985; Tailor and McLennan, 1985). In the plot Sc/Cr versus La/Y (Fig 18; Bhatia and Crook, 1986) the Kopili sandstones

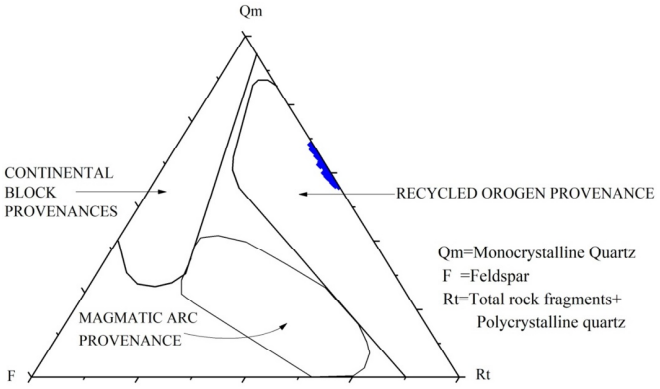

Fig. 16. Triangular plots of Qm-F-Rt showing tectono-provenance of the Kopili Sandstones (after Dickinson and Suczek 1979)

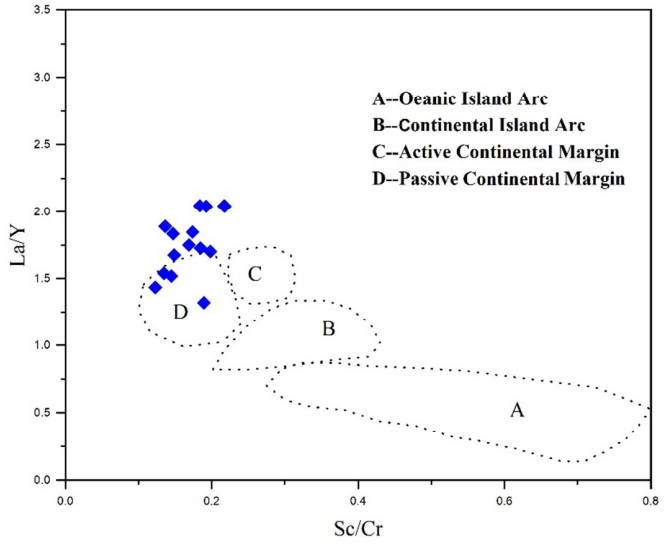

Fig.17. Bivariate plot of Sc/Cr vs La/Y of the Kopili sandstones showing tectonic setting (after Bhatia and Crook, 1986).

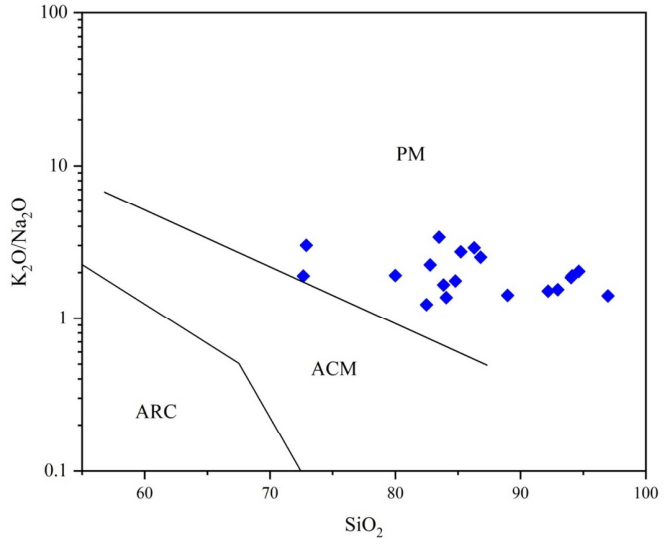

Fig. 18. Bivariate plot of K_2O/Na_2O vs SiO_2 of the Kopili sandstones showing Tectonic setting (after Roser and Korsch, 1986).

show some scattering but most of the samples fall within the passive continental margin. In the major element-based discrimination diagram of Verma and Armstrong-Altrin (2013) for high silica-rich sediments (Fig. 19), the majority of the studied Kopili samples are plotted in the rift-related environment (except one sample). The trace element based ternary diagrams i.e., Th-Co-Zr/10 and Th - Sc - Zr/10 (Bhatia and Crook 1986, Fig. 20a & b) diagrams also support the major element-based observation.

CONCLUSION

- Kopili sandstones are classified as quartz arenite to sublitharenite and arkose to sublitharenite as per petrography and major element geochemistry respectively. The sandstones are highly matured.
- Weathering indices, CIA, CIW, PIA and A - CN - K diagram characterized Kopili sandstones as low to moderately weathered (except 49D sample) under arid to semi humid climatic conditions.
- The major element-based discrimination function diagrams, trace elements (including REEs) and their ratios (Eu/Eu*, La/Sc, Th/

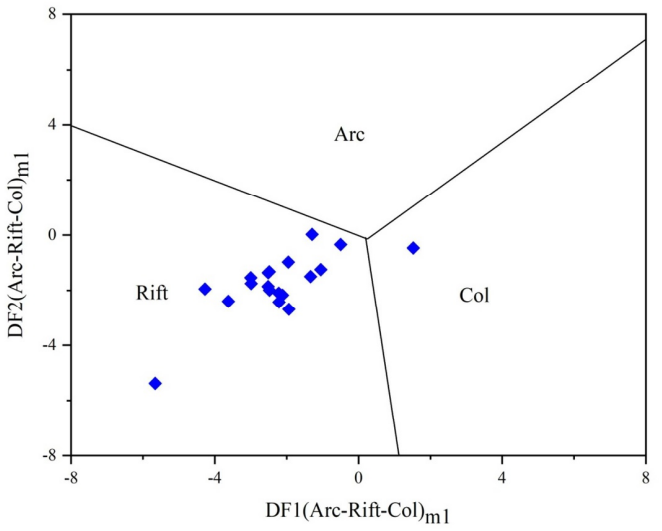

Fig.19. Discrimination diagram for the silica rich Kopili sediments (Verma and Armstrong - Altrin, 2013); DF1(Arc-Rift-Col)m1=(0.263× ln (TiO_2/SiO_2)adj)+ (0.604× ln (Al_2O_3/SiO_2) adj)+ (-1.725× ln (Fe_2O_3/SiO_2) adj)+ (0.660× ln (MnO/SiO_2) adj)+ (2.191× ln (MgO/SiO2) adj)+ (0.144× ln (CaO/SiO_2) adj)+ (-1.304× ln (Na_2O/SiO_2) adj)+ (0.054× ln (K_2O/SiO_2) adj)+ (-0.330× ln (P_2O_5/SiO_2) adj)+ 1.588; DF2 (Arc-Rift-Col)m1=(-1.196× ln (TiO_2/SiO_2) adj)+ (1.064× ln(Al_2O3/SiO_2) adj)+ (0.303× ln (Fe_2O_3/SiO_2) adj)+ (0.436× ln (MnO/SiO_2) adj)+ (0.838× ln (MgO/SiO_2) adj)+ (-0.407× ln (CaO/SiO_2) adj)+ (1.021× ln (Na_2O/SiO_2) adj)+ (-1.706× ln (K_2O/SiO_2) adj)+(-0.126× ln (P_2O_5/SiO_2) adj)- 1.068.

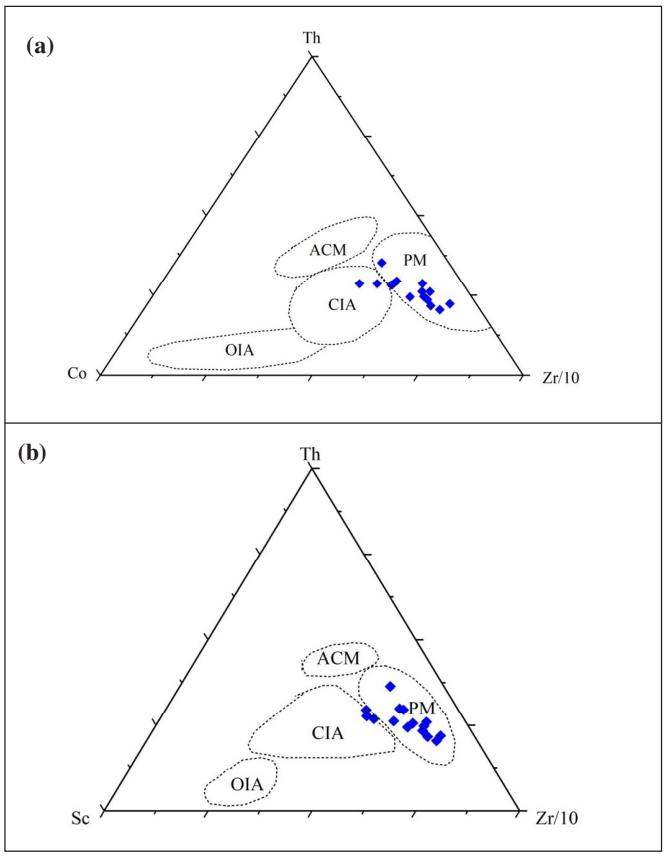

Fig. 20. (a), (b). Tectonic setting discrimination plots for the Kopili sandstones (after Bhatia and Crook,1986); OIA- oceanic island arc; CIA- continental island arc; ACM- active continental margin; PM- passive margin.

Sc, Th/Co, La/Co and Th/Cr) indicate felsic dominant source for the Kopili sandstone.

- Based on detrital modes and major and trace element diagrams it has been suggested that the Kopili sandstone is deposited in a passive continental margin setting.

Acknowledgement: The authors are thankful to the CSIR-National Geophysical Research Institute, Hyderabad for extending laboratory facilities for geochemical analyses. The authors are also grateful to the Department of Science and Technology, Govt. of India for enhancing laboratory facilities in the Department of Geological Sciences, Gauhati University through the FIST-2016 grant that offered immense help in petrographical analysis of the samples.

References

Absar, N., Nizamudheen, B. M., Augustine, S., Managave, S. and Balakrishnan, S. (2016) C, O, Sr and Nd isotope systematics of carbonates of Papaghni sub-basin, Andhra Pradesh, India: Implications for genesis of carbonate-hosted stratiform uranium mineralization and geodynamic evolution of the Cuddapah Basin. Lithos, v.263, pp.88-100.

Armstrong-Altrin, J. S. (2009) Provenance of sands from Cazones, Acapulco, and Bahía Kino beaches, Mexico. Revista Mexicana de Ciencias Geologicas, v.26, pp.764-782.

Armstrong-Altrin, J. S., Lee, Y. I., Verma, S. P., and Ramasamy, S. (2004) Geochemistry of sandstones from the Upper Miocene Kudankulam Formation, Southern India: Implications for provenance, weathering, and tectonic setting. Jour. Sediment. Res., v.74, pp.285-297.

Armstrong-Altrin, J. S., Nagarajan, R., Madhavaraju, J., Rosalez-Hoz, L., Lee, Y. I., Balaram, V., Cruz-Martinez, A. and Avila-Ramirez, G. (2013) Geochemistry of the Jurassic and upper Cretaceous shales from the Molango Region, Hidalgo, Eastern Mexico: Implications of source-area weathering, provenance, and tectonic setting. Comptes Rendus Geoscience, v.345, pp.185-202.

Basu, A., Young, S., Suttner, L. J., James, W. C., Mack, C. H. (1975) Re-evaluation of the use of undulatory extinction and polycrystallinity in detrital quartz for provenance interpretation. Jour. Sediment. Petrol., v.45, pp.873-882.

Bauluz, B., Mayayo, M. J., Fernandez-Nieto, C. and Lopez, J. M. G. (2000) Geochemistry of Precambrian and Paleozoic siliciclastic rocks from the Iberian Range (NE Spain): implications for source-area weathering, sorting, provenance, and tectonic setting. Chemical Geol., v.168, pp.135-150.

Bhandari, L.L., Fuloria, R.C. and Sastry, V.V. (1973) Stratigraphy of Assam Valley, India. AAPG Bull., v.57, pp.640-650.

Bhatia, M.R. (1983) Plate tectonics and geochemical composition of sandstone. Jour. Geol., v.91, pp.611- 627.

Bhatia, M.R. and Crook, K.A.W. (1986) Trace element characteristics of greywackes and tectonic setting discrimination of sedimentary basins. Contrib. Mineral. Petrol., v.92, pp.181-193.

Chakraborty, A., Mitra, P., Chakraborty, D.K. and Ramdev, C.M. (1974) Geology of Tertiary sedimentary belts of Garo and Khasi hills, Meghalaya. ONGC Report (Unpublished).

Condie, K.C. (1993) Chemical composition and evolution of the upper continental crust; Contrasting results from surface samples and shales. Chemical Geol., v.104, pp.1-37.

Cox, R. and Lowe, D.R. (1995) A conceptual review of regional scale controls on the composition of clastic sediment and the coevolution of continental blocks and their sedimentary cover. Jour. Sediment. Res., v.65, pp.1-12.

Crook, K.A.W. (1974) Lithogenesis and geotectonics: the significance of compositional variation in flysch arenites (graywackes), *In:* Dott, R.H. and Shaver, R.H. (Eds.), Modern and ancient geosynclinal sedimentation: SEPM Spec. Publ., no.19, pp.304-310.

Cullers, R. L. and Podkovyrov, V.N. (2000) Geochemistry of the Mesoproterozoic Lakhanda shales in southern Yakutia, Russia: Implications for mineralogical and provenance control, and recycling. Precambrian Res., v.104, pp.77-93.

Cullers, R.L., (2000) The geochemistry of shales, siltstones, and sandstones of Pennsylvanian-Permian age, Colorado, USA: Implications for provenance and metamorphic studies. Lithos v.51, pp.181-203.

Cullers, R.L., Chaudhuri, S., Kilbane, N. and Koch, R. (1979) Rare earths in size fractions and sedimentary rocks of Pennsylvanian Permian age from the mid-continent of the U.S.A. Geochim. Cosmochim. Acta, v.43, pp.1285-1302.

Dabard, M.P. (1990) Lower Brioverian Formation (Upper Proterozoic) of the American Massif (France): Geodynamic evolution of source areas revealed by sandstone petrography and geochemistry. Sediment. Geol., v.69, pp.45-8.

Deshpande, S. V., Goel, S. M, Bhandari, A., Baruah, R.M., Deshpande, J.S, Kumar, A., Rana, K.S, Chitrao, A.M., Giridhar, M., Chowdhuri, D., Kale, A.S and Phor, L. (1993) Lithostratigraphy of Indian petroliferous basins: Document-X. Unpublisd Report, ONGC.

Dickinson, W.R. and Suczek, C.A. (1979) Plate tectonics and sandstone compositions. AAPG Bull., v.63, pp.2164-2182

Dickinson, W.R., Beard, L.S., Brakenridge, G.R., Erjavec, J.L., Ferguson, R.C., Inman, K.F., Knepp, R.A., Lindberg, F.A. and Ryberg, P.T. (1983) Provenance of North American Phanerozoic sandstones in relation to tectonic setting. Geol. Soc. Amer. Bull., v.94, pp.222-235.

Dickinson, W.R. Bear, L.S., Brakenridge, Erjavec, J.L., Ferguson, R.C., Inman, K.F., Knepp, R.A. Lindberg, F.A. and Ryberg, P.T. (1983) Provenance of North American Phanerozoic sandstones in relation to tectonic setting. Geol. Soc. Amer. Bull., v.94, pp.222-235.

Dutta, S.K. and Jain, K.P. (1980) Geology and palynology of the area around Lumshnong, jaintia Hills. Meghalaya, India. Biological Memoirs, v.5, pp.56-81.

Evans, P. (1932) The Tertiary succession in Assam: Geology and Metallurgy Institute of India. Trans. Mineral., v.27, pp.155-260.

Fatima, S. and Khan, M.S. (2012) Petrographic and geochemical characteristics of Mesoproterozoic Kumbalgarh clastic rocks, NW Indian shield: Implications for provenance, tectonic setting and crustal evolution. Internat. Geol. Rev., v.54, pp.1113-1144.

Fedo, C.M. Wayne Nesbitt, H., and Young, G.M. (1995) Unraveling the effects of potassium metasomatism in sedimentary rocks and paleosols, with implications for paleoweathering conditions and provenance. Geology, v.23, pp.921-924.

Feng, R. and Kerrich, R. (1990) Geochemistry of fine grained clastic sediments in the Archaean Abitibi Greenstone Belt, Canada: Implications for provenance and tectonic setting. Geochim. Cosmochim. Acta, v.54, pp.1061-1081.

Folk, R.L. (1980) Pertrology of sedimentary rocks. Hemphill Publishing Company, Austin, Texas, U.S.A, pp.182.

Ghosh, S., Sarkar, S., and Ghosh, P. (2012) Petrography and major element geochemistry of the Permo-Triassic sandstones, Central India: Implications for provenance in an intracratonic pull-apart basin. Jour. Asian Earth Sci., v.43, pp.207-240.

Gogoi, A., and Bhagabaty, B. (2018) Geochemical Characteristics of Metasomatised Diorites in and around Umsopri of Ri-bhoi District, Meghalaya. Indian Jour. Geogra., Environ. Earth Sci. Internat., v.15, pp.1-14.

Hara, H., Kunii, M., Hisada K., Ueno, K., Kamata, Y., Srichan, W., Charusiri, P., Charoentitirat, T., Watarai, M., Adachi, Y. and Kurihara, T. (2012) Petrography and geochemistry of clastic rocks within the In-thanon zone, northern Thailand: Implications for Paleo-Tethys subduction and convergence. Jour. Asian Earth Sci., v.61, pp.2-15.

Hayashi, K., Fujisawa, H., Holland, H. D. and Ohmoto, H. (1997) Geochemistry of ~1.9 Ga sedimentary rocks from Northeastern Labrador, Canada. Geochim. Cosmochim. Acta, v.61, pp.4115-4137.

Hofmann, A. (2005) The geochemistry of sedimentary rocks from the Fig Tree Group, Barberton Greenstone Belt: Implications for plate tectonic, hydrothermal and surface processes during mid-Archean times. Precambrian Res., v.143, pp.23-49.

Hussain, M.F., Islam, M.S., and Deb, M. (2020) Petrological and geochemical study of the Sylhet Trap basalts, Shillong plateau, N.E. India: Implications for petrogenesis. European Jour. Geosci., v.02, pp.01-18.

Ingersoll, R. V., Bullard, T. F., Ford, R. L., Grimm, J. E, Pickle, J. D. and Sares, S. W. (1984) The effect of grain size on detrital modes: a test of the Gazzi-Dickinson point counting method. Jour. Sediment. Petrol., v.54, pp.103-116.

Johnsson, M.J. (1993) The system controlling the composition of clastic sediments. In processes controlling the composition of clastic sediments. *In:* Johnsson M.J. and Basu A. (Eds), Processes controlling the composition of clastic sediments. Geol. Soc. Amer., Spec. Papers 284, pp.1-19.

Khan, T. and Khan, M.S. (2015) Clastic rock geochemistry of Punagarh Basin, Trans-Aravalli region, NW Indian shield: Implications for paleoweathering, provenance, and tectonic setting. Arabian Jour. Geosci., v.8, pp.3621-3644.

Khan, T. and Khan, M.S. (2016) Geochemistry of the sandstones of Punagarh basin: Implications for two source terranes and Arabian-Nubian connection of Aravalli craton? Jour. Geol. Soc. India, v.88, pp.366-386.

Khan, T., Sarma, D.S., and Khan, M.S. (2020) Geochemical study of the Neoproterozoic clastic sedimentary rocks of the Khambal Formation (Sindreth Basin), Aravalli Craton, NW Indian Shield: Implications for paleoweathering, provenance and geodynamic evolution. Geochemistry, v.80, pp.125596.

Khan, T., Sarma, D. S., Somasekhar, V., Ramanaiah, S., and Reddy, N. R. (2019) Geochemistry of the Palaeoproterozoic quartzites of Lower Cuddapah Supergroup, South India: Implications for the palaeoweathering, provenance and crustal evolution. Geol. Jour., v.55, pp.1567-1611.

Krishna, A.K., Murthy, N.N., and Govil, P.K. (2007) Multi element analysis of soils by wavelength-dispersive X-ray fluorescence spectrometry. Atomic Spectroscopy, v.28, pp.202-214.

Krynine, P. D. (1940) Petrology and genesis of the Third Bradford sand, Pennsylvania State College Bulletin, Mineral Industries Experiment Station, Bulletin 29, 134p.

Mackenzie, F.T. and Garrels, R.M. (1971) Evolution of sedimentary rocks. Norton, New York.

McLennan, S.M. (1989) Rare earth elements in sedimentary rocks; influence of provenance and sedi-mentary processes. *In:* Lipin, B.R. and McKay, G. A. (Eds.), Rev. Mineral. Geochem., v.21(1), pp.169-200.

McLennan, S.M. (1989) Rare earth elements in sedimentary rocks; influence of provenance and sedimentary processes. Rev. Mineral., v.21, pp.169-200.

McLennan, S.M., Hemming, S., McDaniel, D.K. et al. (1993) Geochemical approaches to sedimentation, provenance, and tectonics. Spec. Papers Geol. Soc. Amer., v.284, pp.21-44.

McLennan, S.M., Taylor, S.R., McCulloch, M.T. and Maynard, J.B. (1990) Geochemical and Nd-Sr iso-topic composition of deep-sea turbidites: Crustal evolution and plate tectonic associations. Geo-chim. Cosmochim. Acta, v.54, pp.2015-2050.

Medlicott, H.B. (1869) Geological sketch of the Shillong Plateau in N-E Bengal. Memoirs of the Geol. Surv. India, v.7, pp.151-207.

Nesbitt, H.W. and Young, G. M. (1982) Early Proterozoic climates and plate motions inferred from ma-jor element chemistry of lutites. Nature, v.299, pp.715-717.

Nesbitt, H.W. and Young, G.M. (1984) Prediction of some weathering trends of plutonic and volcanic rocks based on thermodynamic and kinetic considerations. Geochim. Cosmochim. Acta, v.48, pp.1523-1534.

Nesbitt, H.W. and Young, G.M. (1989) Formation and diagenesis of weathering profiles. Jour. Geol., v.97, pp.129-147.

Nesbitt, H.W., Markovics, G. and Price, R.C. (1980) Chemical processes affecting alkalis and alkaline earths during continental weathering. Geochim. Cosmochim. Acta, v.44, pp.1659-1666.

Nesbitt, H.W., Young. G.M., McLennan, S.M. and Keays, R.R. (1996) Effect of geochemical weathering and sorting on the petrogenesis of siliciclastic sediments, with implications for provenance studies. Jour. Geol., v.104, pp.525-542.

Nesbitt, H.W., Markovics, G. and Price, R.C. (1980) Chemical processes affecting alkalis and alkaline earths during continental weathering. Geochim. Cosmochim. Acta, v.44, pp.1659-66.

Periasamy, V., and Venkateshwarlu, M. (2017) Petrography and geochemistry of Jurassic sandstones from the Jhuran Formation of Jara dome, Kachchh basin, India: Implications for provenance and tectonic setting. Earth System Science, v.126, pp.44.

Perri, F., Critelli, S., Cavalcante, F., Mongelli, G., Dominici, R., Sonnino, M. and De Rosa, R. (2012) Provenance signatures for the Miocene volcaniclastic succession of the Tufiti di Tusa Formation, south-ern Apennines, Italy. Geol. Magz., v.149, pp.423-442.

Pettijohn, F.J. (1975) Sedimentary Rocks. 3rd Edition, Harper and Row, New York, 628p.

Pettijohn, F.J., Potter, P.E., and Siever, R. (1972) Sand and Sandstones. Springer, Berlin Heidelberg, New York, 618p.

Pettijohn, F.J., Potter, P.E., and Siever, R. (1987) Sand and Sandstone. Springer, pp.431-487.

Potter, P.E., Maynard, J.B. and Depetris, P.J. (2005) Mud and mudstones: Introduction and overview. Springer, Heidelbeerg, 297p.

Ray, J., Saha, A., Ganguly, S., Balaram, V., Krishna, A.K. and Hazra, S. (2011) Geochemistry and petrogenesis of Neoproterozoic Mylliem granitoids, Meghalaya Plateau, Northeastern India. Earth System Science, v.120, pp.459-473.

Reddy, A.N., Nayak, K.K., Gogoi, D. and Satyanarayana, K. (1992) Trace fossils in cores of Kopili, Barail and Tipam sediments of Upper Assam Shelf. Jour. Geol. Soc. India, v.40(3), pp.253-257.

Roddaz , M., Debat, P. and Nikiema, S. (2007) Geochemistry of upper Birimian sediments (major and trace elements and Nd-Sr isotopes) and implications for weathering and tectonic setting of the late Palaeoproterozoic crust. Precambrian Res., v.159, pp.197-211.

Roser, B. P. and Korsch, R. J. (1986) Determination of tectonic setting of sandstone-mudstone suites using SiO_2 content and K_2O/Na_2O ratio. Jour. Geol., v.94, pp.635-650.

Roser, B.P. and Korsch, R.J. (1988) Provenance signatures of sandstone-mudstone suites determined using discriminant function analysis of major-element data. Chemical Geol., v.67, pp.119-139.

Roser, B.P. and Korsch, R.J. (1985) Plate tectonics and geochemical composition of sandstones: a discussion. Jour. Geol., v. 93, pp. 81- 84.

Roy Moulik, S.K., Singh, H.J., Singh Rawat, R.K., Akhtar, S.M., Mayor, S. and Asthana, M. (2009) Sand Distribution Pattern and Depositional Model of Kopili Formation (Eocene) with Special Reference to Sequence Stratigraphic Framework from North Assam Shelf, Assam-Arakan Basin, India. Search and Discovery Article 50196, AAPG Annual Convention, Colorado.

Samanta, B.K. (1968) Nummulites (foraminifera) from the Upper Eocene Kopili Formation of Assam, India. Paleontol., v.11, pp.669-682.

Samanta, B.K. (1985) Pellatispira (Foraminiferida) from the Upper Eocene Kopili Formation of Garo Hills, Meghalaya. Jour. Geol. Soc. India, v.26, pp.199-207.

Satyanarayanan, M., Balaram, V., Sawant, S. S., Subramanyam, K. S. V., and Krishna, G. V. (2014) High precision multielement analysis on geological samples by HR?ICPMS. Proceeding of 28th ISMAS symposium Cum Workshop on Mass Spectrometry, Indian Society for Mass Spectrometry, Mum-bai, pp.181?184.

Saxena, R.K. and Trivedi, G.K. (2009) Palynological investigation of the Kopili Formation (Late Eocene) in North Cachar Hills, Assam, India. Acta Palaeobotanica, v.49, pp.253-277.

Sein, M.K. and Sah, S.C.D. (1974) Palynological demarcation of the Eocene-Oligocene sediments in the Jowai-Badarpur Road Section, Assam. Proceeding of Symposium on Stratigraphical Palynology, Lucknow, 1971, Special Publication 3, Birbal Sahni Institute of Palaeobotany, Lucknow, pp. 99-105.

Sheldon, N.D., Retallack, G.J. and Tanaka, S. (2002) Geochemical climofunctions from North American soils and application to paleosols across the Eocene-Oligocene boundary in Oregon. Jour. Geol., v.110, pp.687-696.

Sun, S.S. and McDonough, W.F. (1989) Chemical and isotopic systematics of oceanic basalts: implica-tions for mantle compositions and Processes. *In:* Saunders, A.D., Norry, M.J. (Eds.), Magmatism in the Ocean Basins. Geol. Soc. London, Spec. Publ., v.42, pp.315-345.

Suttner, L.J. and Dutta, P.K. (1986) Alluvial sandstone composition and palaeoclimate framework mineralogy. Jour. Sediment. Petrol., v.56, pp.329-345.

Taylor, S.R. and McLennan, S.M. (1985) The Continental Crust: Its Composition and Evolution. Blackwell Scientific, Oxford, 312p.

Tripathi, S.K.M. and Singh, H.P. (1984) Palynostratigraphical zonation and correlation of the Jowai-Badarpur Road Section (PalaeoceneEocene), Meghalaya. India. Proceeding of the 5th Indian Ge-ophytological Conference. Palaeobotanical Soc., Lucknow, pp.316- 328.

Trivedi, G.K. and Ranhotra, P.S. (2015) Palynofloral evidence for palaeoecology and depositional environment of the Kopili Formation (Late Eocene), Jaintia Hills, Meghalaya. Jour. Geol. Soc. India, v.86, pp.33-40.

Van de Kamp, P. C. and Leake, B. E. (1985) Petrography and geochemistry of feldspathic and mafic sediments of the northeastern Pacific margin; Earth and Environmental Science. Trans. Royal Soc. Edinburg, v.76, pp.411-449.

Verma, S.P. and Armstrong-Altrin, J.S. (2013) New multi-dimensional diagrams for tectonic discrimination of siliciclastic sediments and their application to Precambrian basins. Chemical Geol., v. 355, pp.117-133.

Walsh, J.P., Wiberg, P.L., Aalto R., Nittrouer, C.A. and Kuehl, S. A. (2016) Source-to-sink research: Ecoomy of the Earth's surface and its strata. Earth Sci. Rev., v.153, pp.1-6.

Zaidi, S. and Chakrabarti, S. K. (2006) Sequence stratigraphy and depositional environment of the Kopili Formation in the area between Borholla and Khoraghat, Dhansiri Valley, South Assam Shelf. Proceedings of 6th International Conference and Exposition on Petroleum Geophysics, Kolkata, pp.652-661.